justed to meet the requirements of the digestion apparatus used.]

An example procedure that has been shown to have broad applicability is the following. Dehydrate and predigest 0.5 g of primary sample in 5 mL of freshly prepared *Concentrated Acid.* Allow to sit loosely covered for 30 minutes in a fume hood. Add an additional 10 mL of *Concentrated Acid,* and digest, using a closed vessel technique, until digestion or extraction is complete. Repeat if necessary by adding an additional 5 mL of *Concentrated Acid.* [NOTE—Where closed vessel digestion is necessary, follow the manufacturer's recommended procedures to ensure safe use.]

Reagents: All reagents used for the preparation of sample and standard solutions should be free of elemental impurities, in accordance with *Plasma Spectrochemistry* ⟨730⟩.

Procedure 1: ICP-AES

Standardization solution 1: *2J* of the *Target Element(s)* in a *Matched Matrix*

Standardization solution 2: 0.5*J* of the *Target Element(s)* in a *Matched Matrix*

Sample stock solution: Proceed as directed in *Sample Preparation* above. Allow the sample to cool, if necessary. For mercury determination, add an appropriate stabilizer.

Sample solution: Dilute the *Sample Stock Solution* with an appropriate solvent to obtain a final concentration of the *Target Elements* at NMT *2J.*

Blank: *Matched Matrix*

Elemental spectrometric system
(See *Plasma Spectrochemistry* ⟨730⟩.)

Mode: ICP

Detector: Optical detection system

Rinse: Diluent used

Standardization: *Standardization solution 1, Standardization solution 2,* and *Blank*

System suitability

Sample: *Standardization solution 1*

Suitability requirements

Drift: Compare results obtained from *Standardization solution 1* before and after the analyis of the *Sample solutions.*

Suitability criteria: NMT 20% for each *Target Element.* [NOTE—If samples are high in mineral content, rinse system well (60 seconds) before introducing the *Sample* in order to minimize carryover.]

Analysis: Analyze according to the manufacturer's suggestions for program and wavelength. Calculate and report results on the basis of the original sample size. [NOTE—Appropriate measures must be taken to correct for matrix-induced interferences (e.g., Wavelength overlaps).]

Procedure 2: ICP-MS

Standardization solution 1: *2J* of the *Target Element(s)* in a *Matched Matrix*

Standardization solution 2: 0.5*J* of the *Target Element(s)* in a *Matched Matrix*

Sample stock solution: Proceed as directed for *Sample Preparation* above. Allow the sample to cool, if necessary. For mercury determination, add an appropriate stabilizer.

Sample solution: Dilute the *Sample stock solution* with an appropriate solvent to obtain a final concentration of the *Target Elements* at NMT *2J.*

Blank: *Matched Matrix*

Elemental spectrometric system
(See *Plasma Spectrochemistry* ⟨730⟩.)

Mode: ICP. [NOTE—An instrument with a cooled spray chamber is recommended. (A collision cell or reaction cell may also be beneficial.)]

Detector: Mass spectrometer

Rinse: Diluent used

Standardization: *Standardization solution 1, Standardization solution 2,* and *Blank*

System suitability

Sample: *Standardization solution 1*

Suitability requirements

Drift: Compare results obtained from *Standardization solution 1* before and after the analysis of the *Sample solutions.*

Suitability criteria: *Drift* NMT 20% for each *Target Element.* [NOTE—If samples are high in mineral content, rinse system well (60 seconds) before introducing the *Sample* in order to minimize carryover.]

Analysis: Analyze according to the manufacturer's suggestions for program and *m/z.* Calculate and report results based on the original sample size. [NOTE—Appropriate measures must be taken to correct for matrix-induced interferences (e.g., argon chloride interference with arsenic determinations.]

ALTERNATE PROCEDURE VALIDATION

If a specified compendial procedure does not meet the needs of a specific application, an alternative procedure may be used (see *General Notices* 6.30). Alternative procedures must be validated and must be acceptable and therefore equivalent to the compendial procedures for the purposes of the test. The principles of validation are provided in general chapter *Validation of Compendial Procedures* ⟨1225⟩. The level of validation necessary to ensure that an alternative procedure is acceptable depends on whether a limit test or a quantitative determination is necessary. The requirements for validation of an elemental impurities procedure for either type of determination are described below. Where this information differs from that presented in *Validation of Compendial Procedures* ⟨1225⟩, the parameters and acceptance criteria presented in this chapter take precedence. Any alternative procedure that has been validated and meets the acceptance criteria that follow is considered to be equivalent to the compendial procedures for the purposes of this test.

LIMIT PROCEDURES

The following section defines the validation parameters for the acceptability of alternative limit procedures. Meeting these requirements must be demonstrated experimentally using an appropriate system suitability procedure and reference material. Meeting these requirements demonstrates that the procedure is equivalent to the compendial procedure as a limit procedure for the *Target Element.*

The suitability of the method must be determined by conducting studies with material or mixture under test supplemented with known concentrations of each *Target Element* of interest at the appropriate acceptance limit concentration. The material or mixture under test must be spiked before any sample preparation steps are performed.

Detectability

Standard solution: A preparation of reference materials for the *Target Element(s)* at the *Target Concentrations.*

Spiked sample solution 1: Prepare a solution of sample under test, spiked with appropriate reference materials for the *Target Elements* at the *Target Concentration,* solubilized or digested as described in *Sample Preparation.*

Spiked sample solution 2: Prepare a solution of the sample under test, spiked with appropriate reference materials at 80% of the *Target Concentration* for the *Target Elements*, solubilized or digested as described in *Sample Preparation*.

Unspiked sample solution: A sample of material under test, solubilized or digested in the same manner as the *Sample solutions*.

Acceptance criteria

Non-instrumental procedures: *Spiked sample solution 1* provides a signal or intensity equivalent to or greater than that of the *Standard Solution*. *Spiked sample solution 2* must provide a signal or intensity less than that of the *Spiked sample solution 1*. [NOTE—The signal from each *Spiked sample solution* is NLT the *Unspiked sample solution* determination.]

Instrumental procedures: The average value of the three replicate measurements of *Spiked sample solution 1* is within (±15%) of the average value obtained for the replicate measurements of the *Standard solution*. The average value of the replicate measurements of *Spiked sample solution 2* must provide a signal intensity or value less than that of the *Standard solution*. [NOTE—Correct the values obtained for each of the spiked solutions using the *Unspiked sample solution*.]

Precision for Instrumental Methods (Repeatability)

[NOTE—Non-instrumental precision is demonstrated by meeting the *Detectability* requirement above.]

Sample solutions: Six independent samples of the material under test, spiked with appropriate reference materials for the *Target Elements* at the *Target Concentration*.

Acceptance criteria

Relative standard deviation: NMT 20% for each *Target Element*.

Specificity

The procedure must be able to unequivocally assess (see *Validation of Compendial Procedures* ⟨1225⟩) each *Target Element* in the presence of components that may be expected to be present, including other *Target Elements*, and matrix components.

QUANTITATIVE PROCEDURES

The following section defines the validation parameters for the acceptability of alternative quantitative procedures. Meeting these requirements must be demonstrated experimentally, using an appropriate system suitability procedure and reference materials. Meeting these requirements demonstrates that the procedure is equivalent to the compendial procedure for the purpose of quantifying the *Target Elements*.

Accuracy

Standard solutions: Prepare solutions containing the *Target Elements* at concentrations ranging from 50% to 150% of *J*, using appropriate reference materials.

Test samples: Prepare samples of the material under test spiked with appropriate reference materials before any sample preparation steps (digestion or solubilization) at concentrations ranging from 50% to 150% of *J* for each *Target Element*.

Acceptance criteria

Spike recovery: 70%–150% for the mean of three replicate preparations at each concentration

Precision

REPEATABILITY

Test samples: Six independent samples of material under test (taken from the same lot) spiked with appropriate reference materials for the *Target Element(s)* at the indicated level.

Acceptance criteria

Relative standard deviation: NMT 20% for each *Target Element*

RUGGEDNESS

Perform the *Repeatability* analysis over three independent events using the following events or combinations thereof:

1. on different days, or
2. with different instrumentation, or
3. with different analysts.

Acceptance criteria

Relative standard deviation: NMT 25% for each *Target Element*

Specificity

The procedure must be able to unequivocally assess (see *Validation of Compendial Procedures* ⟨1225⟩) each *Target Element* in the presence of components that may be expected to be present, including other *Target Elements*, and matrix components.

Limit of Quantitation, Range, and Linearity

Demonstrated by meeting the *Accuracy* requirement.

■2S (USP35)

厚生労働科学研究費補助金　（医薬品・医療機器レギュラトリーサイエンス総合研究事業）
分担研究報告書

製剤および製剤試験法の改正に関する研究
－タンパク質製剤における凝集体解析法－

研究代表者　川西　徹（国立医薬品食品衛生研究所）
研究協力者　新見伸吾　（国立医薬品食品衛生研究所　生物薬品部）
研究協力者　遠藤素子　（国立医薬品食品衛生研究所　生物薬品部）

研究要旨

抗体医薬品原薬の製造工程と最終製品における凝集体の相対レベルの推定における動的光散乱の有用性を評価するために，ヒト化抗体医薬品製剤を攪拌することにより誘導した凝集体と単量体の粒子径及び相対光散乱強度を動的光散乱により測定した．

単量体と凝集体の粒子径はそれぞれ5及び500 nmであった．凝集体と単量体を1対6の比で混合すると凝集体の相対光散乱強度は約50%であった．これらの知見は凝集体の相対光散乱強度は単量体に比べ約7倍高いことを示している．したがって，凝集体が1種類であり単量体と凝集体の粒子径とその相対光散乱強度の関係が既に明らかになっている場合，動的光散乱は凝集体の相対含量の推定に有用であることが示唆された．

キーワード：凝集体，ヒト化抗体医薬品製剤，動的光散乱

A. 研究目的

タンパク質性医薬品において，目的物質由来不純物である凝集体は目的物質に比べて活性が低下するだけでなく免疫原性の原因となる可能性が懸念されている[1,2]．例えば，IFN-β製剤では凝集体が通常のマウス及びトランスジェニックマウスにおいて抗体産生を誘導することが知られている[3-5]．また，臨床における抗体の産生頻度と凝集体の割合が相関することも示唆されている[6,7]．したがって，その上限値は可能な限り低く設定し，厳密に管理する必要がある．

しかしながら，高濃度で抗体医薬品を産生すると，小胞体に存在しフォールディングに関与する分子シャペロンに対する抗体医薬品の割合が過剰になり，フォールディングされない抗体医薬品が生じる．その結果，フォールディングされない抗体医薬品より凝集体が誘導され，その割合は最大30%に達する場合がある[8,9]．抗体医薬品の精製工程には，プロテインAクロマトグラフィーで酸性溶液（pH約3）による溶出工程が含まれる．このような極端なpHに抗体医薬品が曝露されると，抗体医薬品の表面及び内部の荷電性極性基（グルタミン酸，アスパラギン酸，リシン，アルギニン，ヒスチジン）の荷電状態が変化する．これによりクーロン相互作用（荷電粒子間に働く

力）によるストレスがかかり，抗体医薬品が変性する．変性した抗体医薬品は凝集体が誘導されやすい[10]．また，1回の投与量が多く一般的に数十 mg/mL の高濃度で処方されるため，製剤化，保存状況下で凝集体がさらに増加する可能性がある[11]．

凝集体の測定には，サイズ排除クロマトグラフィー，超遠心分析法，場流動分画，動的光散乱法，SDS-PAGE，マイクロ・フロー・イメージング等が用いられている[12,13]．その中で，動的光散乱は不溶性の凝集体も含め最大約 5μm の粒子径を有する凝集体を，吸光度の測定と同様な簡単な操作で測定可能であり，用いるサンプルの容量も約 30μL と微量で測定時間も約数分と短い．ダイナミックレンジは他の測定法に比べて広く，希釈せずに測定できるので，凝集体の解離を回避することができる．また，相対光散乱強度は粒子径の 6 乗に比例して増大するため[14]，高感度の測定が可能である．しかし，定量的な関係が成り立つのは球状の場合でのみあり，形状が異なれば相対光散乱強度は異なるため定量的な測定はできない．

我々は抗体医薬品製剤をガラスバイアル中で攪拌することにより，大きな粒子径の凝集体を効果的に誘導できることを見出している[15]．そこで同じ濃度の抗体医薬品製剤の単量体とこの方法で作製した凝集体の溶液を任意の比率で混合して動的光散乱で測定し，凝集体の含量と相対光散乱強度との関係について解析を行なった．

B. 研究方法

1. サンプルの調製

ヒト化モノクローナル抗体製剤溶液を 4 度で保存した．実験開始時に 25mM クエン酸ナトリウム(pH 6.0), 125mM 塩化ナトリウムで 0.1mg/mL に希釈した．

2. 凝集体の誘導

直径 1.4cm のガラスバイアルにサンプル 1.2mL を入れ攪拌子を用いて 250rpm，室温で 2.5 時間攪拌した．コントロールとして攪拌しないサンプルを同様に調製した．

3. 単量体，凝集体，単量体と凝集体の混合物の測定

単量体，凝集体，単量体と凝集体の様々な比の混合物の粒子径(nm)及び相対光散乱強度(%)は Malvern 社の Zetasizer Nano-ZS により測定した．

4. 統計解析

データは Student's t-test を用いて解析した．P 値が 0.05 以下の場合は統計的に有意と考えた．

C. 結果

図 1 に単量体，凝集体及び凝集体と単量体の 1 対 4 の混合物の粒子径及び相対光散乱強度を示す．単量体は粒子径約 5nm の位置に単一のピークを示した．一方，凝集体は粒子径約 500nm の位置に単一のピークを示した．凝集体と単量体の 1 対 4 の混合物における凝集体及び単量体の相対光散乱強度はそれぞれ 61%及び 39%であった．

図 2 に様々な比率の凝集体と単量体混合液における単量体の相対光散乱強度を示す．凝集体に対する単量体の比率を増加させると，凝集体の相対光散乱強度は低下し，1 対 6 の比率で約 50%に低下した．従って，凝集体の相対光散乱強度は単量体に比べ約 7 倍高いことが示された．

D. 考察

凝集体が球状と仮定して算出された粒子径に基づくと，凝集体の相対光散乱強度は単量体に比べて約 10^6 高い値が計算される[14]．しかし，結果は約 7 倍であったことから，凝集体は球状ではないことが示唆された．攪拌により誘導されるモノクローナル抗体の凝集体の形状のマイクロ・フロー・イメージングによる解析では，細長い形状が観察されている[16]．本実験で同様な攪拌により誘導された凝集体も細長い形状をしているため，相対光散乱強度が弱いのかもしれない．

したがって，球状である場合を除き，濃度が未知の単量体と凝集体のタンパク質混合溶液において，動的光散乱により求めた粒子径と相対光散乱強度から凝集体の含量を推定することはできないことが再確認された．

E. 結論

本研究結果より，凝集体が 1 種類の粒子径のものしか存在しない場合，単量体と凝集体の比率を変えて調製した混合溶液における凝集体の相対光散乱強度の検量線から，凝集体含量を推定することが可能であることが示された．今後，抗体医薬品の工程内管理試験及び最終製品における凝集体含量の推定において，このような観点からの動的光散乱の活用が期待される．

F. 参考文献

1) Rosenberg, A.S.: *AAPS J,* 8, (3), E501-507 (2006)

2) Schellekens, H.: *Nephrol Dial Transplant,* 20, Suppl 6, vi3-9 (2005)

3) van Beers, M.M., Sauerborn, M., Gilli, F., Brinks, V., Schellekens, H., Jiskoot, W.: *Pharm Res,* 27, (9) 1812-1824 (2010)

4) Rifkin, R.A. Maggio, E.T. Dike, S. Kerr, D.A. Levy, M.: *J Neuroimmune Pharmacol,* 6,(1), 158-162 (2011)

5) Seefeldt, M.B. Rosendahl, M.S. Cleland, J.L. Hesterberg, L.K.: *Curr Pharm Biotechnol,* 10, (4), 447-455 (2009)

6) van Beers, M.M., Sauerborn, M., Gilli, F., Hermeling, S., Brinks, V., Schellekens, H., Jiskoot, W.: *J Immunol Methods,* 352, (1-2), 32-37 (2010)

7) Bertolotto, A., Deisenhammer, F., Gallo, P., Solberg Sorensen, P.: *J Neurol,* 251, Suppl 2, II15-II24 (2004)

8) Kramarczyk, J.F., Kelley, B.D., Coffman, J.L.: *Biotechnol Bioeng,* 100, (4), 707-720 (2008)

9) Mahler, H.C., Friess, W., Grauschopf, U., Kiese, S.: *J Pharm Sci,* 98, (10), 2909-2934 (2009)

10) Shukla, A.A. Hubbard, B. Tressel, T. Guhan, S. Low, D.: *J Chromatogr B Analyt Technol Biomed Life Sci,* 848, (1), 28-39 (2007)

11) Treuheit, M.J., Kosky, A.A., Brems, D.N.: *Pharm Res,* 19, (4), 511-516 (2002)

12) den Engelsman, J., Garidel, P., Smulders, R., Koll, H., Smith, B., Bassarab, S., Seidl, A., Hainzl, O., Jiskoot, W.: *Pharm Res,* 28, (4), 920-933

13) Narhi, L.O., Jiang, Y., Cao, S.,

Benedek, K., Shnek, D.: *Curr Pharm Biotechnol,* 10, (4), 373-381 (2009)
14) Dynamic Light Scattering: An Introduction in 30 Minutes http://www.malvern.com/common/downloads/campaign/MRK656-01.pdf
15) Niimi, S.: *Kokuritsu Iyakuhin Shokuhin Eisei Kenkyusho Hokoku,* 129, 55-60 (2011)
16)Joubert, M.K., Luo, Q., Nashed-Samuel, Y., Wypych, J., Narhi, L.O.: *J Biol Chem,* 286, (28), 25118-25133 (2011)

G. 健康危険情報

該当しない

H. 研究発表

1. 論文

1) Endo M, Niimi S, Determination of the relative light scattering intensity of aggregates induced by stirring of humanized monoclonal antibody product using dynamic light scattering. Kokuritsu Iyakuhin Shokuhin Eisei Kenkyuusho Hokoku. 2012;(130):43-45

2. 単行本

1) 新見伸吾　第 10 章　バイオ医薬品の凝集体と HCP の免疫原性 バイオ（抗体）医薬品における不純物／凝集の評価・試験と免疫原性，ウイルス安全性への対応　サイエンス&テクノロジー　pp.245-269

2) 新見伸吾，橋井則貴，石井明子，川崎ナナ　第 7 章　抗体医薬品の特性・品質などの評価　抗体医薬品の開発と市場　シーエムシー出版 pp.92-132

3. 講演

1) 新見伸吾　バイオ医薬品の免疫原性のリスク因子の予測・評価方法，有効性及び安全性に及ぼす影響，リスクを低下させるための実践的開発・市販後調査を探る　薬事エキスパート研修会　第 6 回　品質／科学技術特別研修　平成24年9月19, 20日　（大阪，東京）

2) Shingo Niimi Risk factors, clinical consequence and mitigation of immunogenicity. Immunogenicity for Biopharmaceuticals & Biosimilars Asia (16 October 2012 Singapore)

3) 新見伸吾　抗体医薬品（バイオシミラーを含む）の品質評価についてレギュラトリーサイエンス　エキスパート研修会　第 8 回　品質／科学技術特別研修　平成 25 年 3 月 19 日（東京）

I. 知的所有権の取得状況

1. 特許取得

該当しない

2. 実用新案取得

該当しない

3. その他

該当しない

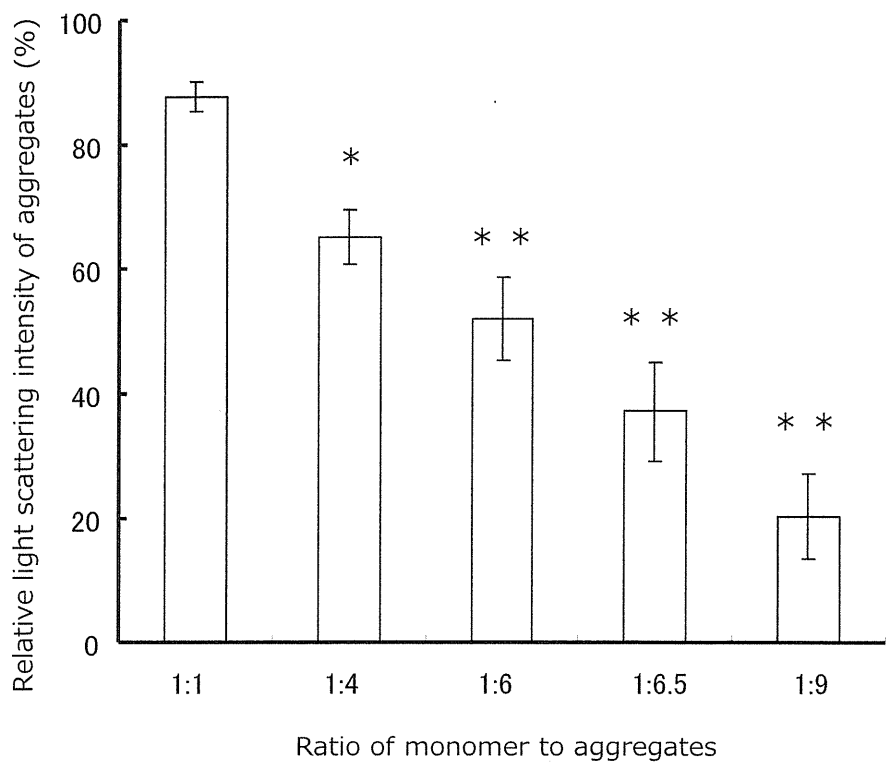

図 2 凝集体と単量体の混合物における凝集体の相対光散乱強度

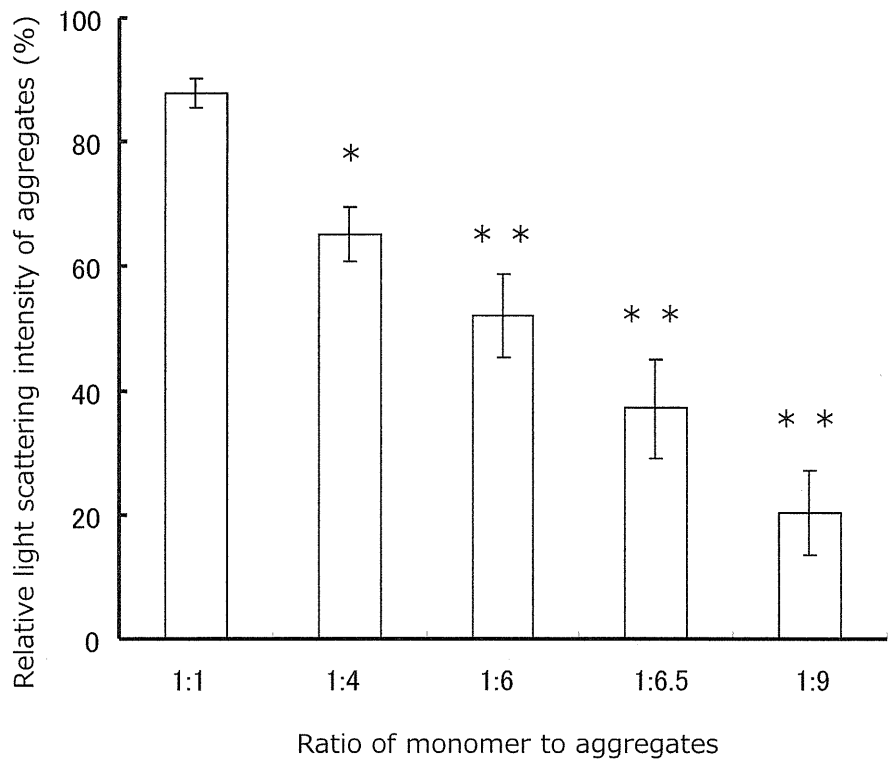

図 2 凝集体と単量体の混合物における凝集体の相対光散乱強度

厚生労働科学研究費補助金（医薬品・医療機器等レギュラトリーサイエンス総合研究事業）
分担研究報告書

医薬品の名称、化学名及び構造式の改正に関する研究

研究分担者　栗原正明　国立医薬品食品衛生研究所　有機化学部長

研究要旨

本研究は、日本薬局方（JP）収載医薬品など、我が国で承認されている医薬品の名称（日本名、英名、別名、）、構造式、分子式、分子量、化学名、ケミカル・アブストラクツ・サービス(CAS)登録番号、および、基原の項に含まれる構造情報などの医薬品の本質を規定する項目（以上を、名称関連事項と略す）について、医薬品の構造・品質管理の高度化と国際化に対応するために必要な検討事項を抽出し、今後のJPの改正作業に資することを目的とする。今年度は日本薬局方名称データベース(JPDB)の構築、管理に関する検討を行った。

A. 研究目的

日本薬局方(JP)には我が国で使用されている主要な医薬品が収載され、法律すなわち規格書としての役割を果たしている。加えてJP は、我が国の医薬品の規範書としての役割も負っている。JP 収載医薬品の医薬品各条は、医薬品の情報記載の規範を示しておりその波及効果は大きい。このような観点から、JP の記載内容は（1）科学的に正しいこと、（2）整合性があること、（3）国際的に調和していること、（4）情報の電子化に対応していることなどが必要条件である。このなかでも特に（3）、（4）の観点から JP のデータベース化は重要である。

B. 研究方法

http://jpdb.nihs.go.jp/jp/に第十六改正日本薬局方名称データベースとして公開している。新規収載品のデータベース上への収載、既収載品の訂正、公開データの拡充、アクセス状況の把握等を行った。

C. 研究結果

【新規収載品のデータベース上への収載】

第一追補収載の 80 品目を追加した。新規収載品を以下に示す。

アシクロビル軟膏、注射用アシクロビル、アゼルニジピン、アムロジピンベシル酸塩口腔内崩壊錠、アルジオキサ顆粒、アルジオキサ錠、イオヘキソール、イオヘキソール注射液、70%一硝酸イソソルビド乳糖末、 一硝酸イソソルビド錠、イブプロフェンピコノール、イブプロフェンピコノールクリーム、イブプロフェンピコノール軟膏、エダラボン、エダラボン注射液、エパルレスタット、エパルレスタット錠、エポエチン アルファ(遺伝子組換え) 、エポエチン ベータ(遺伝子組換え) 、エメダスチンフマル酸塩、エメダスチンフマル酸塩徐放カプセル、オメプラゾール腸溶錠、オーラノフィン、オーラノフィン錠、カルボプラチン、カルボプラチン注射液、クエチアピンフマル酸塩、クエチアピンフマル酸塩細粒、クエチアピンフマル酸塩錠、クロスポビドン、コレスチミド、コレスチミド錠、L－システチン、シンバスタチン錠、セトチアミン塩酸塩水和物、 セフポドキシム プロキセチル錠、タカルシトール水和物、 タカルシトールローション、タルチレリン水和物 タルチレリン錠、タルチレリン口腔内崩壊錠、トラニラスト、トラニラストカプセル、 ト

ラニラスト細粒、 トラニラスト点眼液、シロップ用トラニラスト、 ドルゾラミド塩酸塩、 ドルゾラミド塩酸塩点眼液、 ナルトグラスチム(遺伝子組換え) 、 注射用ナルトグラスチム(遺伝子組換え) 、 ニフェジピン細粒、 ニフェジピン徐放カプセル、 ニフェジピン腸溶細粒 、バルサルタン、バルサルタン錠、ヒプロメロース酢酸エステルコハク酸エステル、 ピロカルピン塩酸塩錠、フィルグラスチム(遺伝子組換え) 、フィルグラスチム(遺伝子組換え)注射液、フェキソフェナジン塩酸塩錠、ブピバカイン塩酸塩水和物、ブロチゾラム、ペミロラストカリウム点眼液、モルヒネ硫酸塩水和物、ラフチジン 、ラフチジン錠、レノグラスチム(遺伝子組換え) 、レボフロキサシン細粒、レボフロキサシン錠、レボフロキサシン点眼液、 ロサルタンカリウム錠、 ロベンザリットナトリウム。
また、以下の４品目を削除した。
注射用アモバルビタールナトリウム、
トリメタジオン錠 、フルラゼパム 、フルラゼパムカプセル。

【データベース記載状況】

日本語版の検索窓を下に示した。

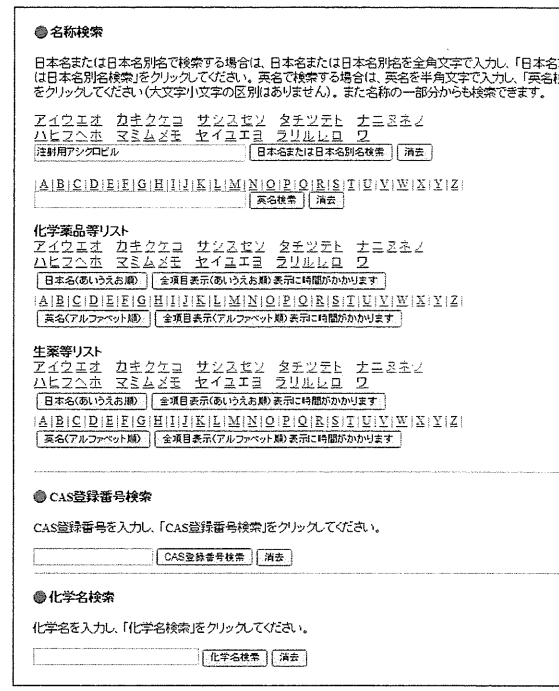

検索できる項目は（1）日本名、日本名別名、英語名、cas 登録番号、化学名検索である。名称の部分検索もできる。

英語版の検索窓を下に示した。

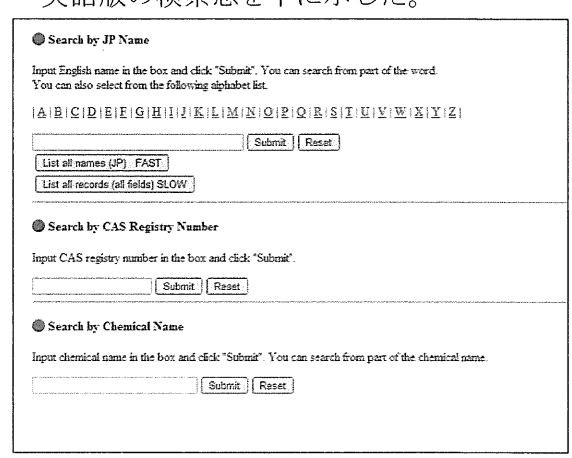

日本名で「トラニラスト」を検索した結果を下に示す。

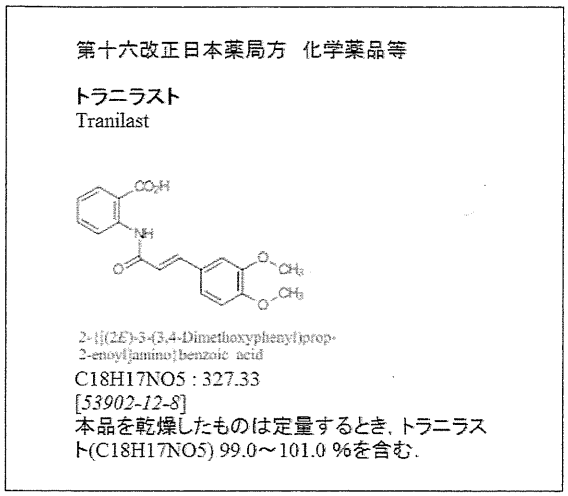
第十六改正日本薬局方　化学薬品等

トラニラスト
Tranilast

2-{[(2*E*)-3-(3,4-Dimethoxyphenyl)prop-2-enoyl]amino}benzoic acid
C18H17NO5 : 327.33
[*53902-12-8*]
本品を乾燥したものは定量するとき，トラニラスト(C18H17NO5) 99.0～101.0 %を含む．

比較のため第十六改正第一追補の冊子体の標記も下に示した。

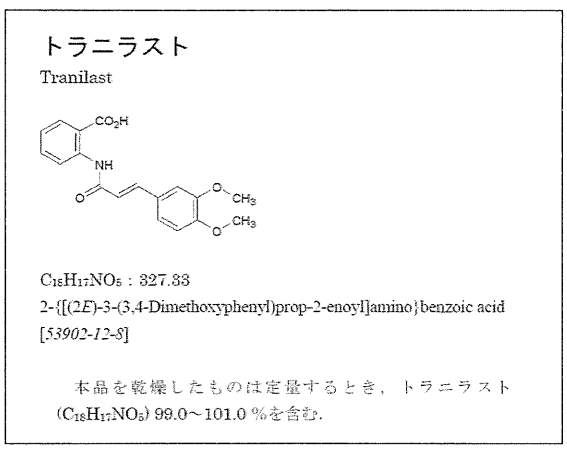
トラニラスト
Tranilast

$C_{18}H_{17}NO_5$: 327.33
2-{[(2*E*)-3-(3,4-Dimethoxyphenyl)prop-2-enoyl]amino}benzoic acid
[*53902-12-8*]

本品を乾燥したものは定量するとき，トラニラスト($C_{18}H_{17}NO_5$) 99.0～101.0 %を含む．

検索結果で表示される情報は、冊子体とほぼ同じ内容になっている。また、データベースの構造式は ChemDraw のファイルとしてダウンロードできる。

【アクセス状況】

2013 年の 1 月 1 日から 3 月 3 1 日までの 3ヶ月間の総アクセス数は 19,228 回であった。1 日の最高アクセス数は 384 件（2013/3/7）であった。

国別のアクセス数を下に示した。

1．	日本国内	18,576
2．	中国	152
3．	米国	98
4．	台湾	89
5．	韓国	58
6．	フランス	52
7．	シンガポール	27
8．	ベトナム	17
9．	インドネシア	16

であった。

【医薬品一般名称データベースとの関連】

国立医薬品食品衛生研究所・有機化学部では、日本薬局方名称データベース（JPDB）の他に医薬品一般名称データベース（JANDB）の構築、管理を行っている。ほぼ共通のフォーマットで構築、管理を行っている。日本薬局方（JP）の収載が決まると医薬品一般名称（JAN）は局方に倣って書き換えられる。

D．考察

データベースの記載内容の拡充が必要である（収載期日等）。現在、日本薬局方名称データベースであるが、構造、名称等の情報だけでなく、より多くの情報を収載する必要があるか検討する必要がある。また、構造ベースの検索ができるようにする検討を行っている。

E．結論

国内外から多くのアクセスがあることより、十分にその機能を果たしていると考えられる。さらに、システム（ハードウエア及びソフトウエア）の見直し、データベースの収載項目、検索項目の充実を図っていく必要がある。

G．研究発表

なし

【参考】

第十六改正日本薬局方名称データベース（JPDB）

http://jpdb.nihs.go.jp/jp/
医薬品一般名称データベース（JANDB）
http://jpdb.nihs.go.jp/jan/

H．知的財産権の出願・登録状況

なし

別紙４

研究成果の刊行に関する一覧表

雑誌

発表者氏名	論文タイトル名	発表誌名	巻号	ページ	出版年
Sakai-Kato K, Ishikura K, Oshima Y, Tada M, Suzuki T, Ishii-Watabe A, Yamaguchi T, Nishiyama N, Kataoka K, Kawanishi T, Okuda H	Evaluation of intracellular trafficking and clearance from HeLa cells of doxorubicin-bound block copolymers.	*Int J Pha*	423	401– 409	2012
Ohno A, Kawanishi T, Okuda H, Fukuhara K.	A new approach to characterization of insulin derived from different species using ^{1}H-NMR coupled with multivariate analysis	*Chem Pharm Bull.*	60	320-324	2012
Sakai-Kato K, Nanjo K, Kawanishi T, Okuda H	Rapid and sensitive method for measuring the plasma concentration of doxorubicin and its metabolites.	*Chem. Pharm. Bull..*	60	391-396	2012
Shibata H, Saito H, Kawanishi T, Okuda H, Yomota C.	Comparison of particle size and dispersion state among commercial cyclosporine formulations and their effects on pharmacokinetics in rats,	*Chem Pharm Bull..*	60	967-975	2012
Shibata H, Saito H, Yomota C, Kawanishi T, Okuda H	Alterations in the detergent-induced membrane permeability and solubilization of saturated phosphatidylcholine/ cholesterol liposomes: effects of poly(ethylene glycol)-conjugated lipid	*Chem Pharm Bull.*	60	1105-1111	2012
Yamaki T, Ohdate R, Nakadai E, Yoshihashi Y, Yonemochi E, Terada K, Moriyama H, Izutsu K, Yomota C, Okuda H, Kawanishi T.	Component crystallization and physical collapse during freeze-drying of L-arginine-citric acid mixtures	*Chem Pharm Bull.*	60	1176-1181	2012

Shibata H, Yomota C, Kawanishi T, Okuda H.	Polyethylene glycol prevents in vitro aggregation of slightly negatively-charged liposomes induced by heparin in the presence of bivalent ions,	*Biol Pharm Bull.*	35	2081-2087	2012
Un K, Sakai-Kato K, Oshima Y, Kawanishi T, Okuda H	Intracellular trafficking mechanism, from intracellular uptake to extracellular efflux, for phospholipid/cholesterol liposomes	*Biomaterials.*	33	8131-8141	2012
Sakamoto T, Portieri A, Arnone D D, Taday P F, Kawanishi T, Hiyama Y	Coating and Density Distribution Analysis of Commercial Ciprofloxacin Hydrochloride Monohydrate Tablets by Terahertz Pulsed Spectroscopy and Imaging	*J Pharm Innov.*	7	87-93	2012
Sakamoto T, Fujimaki Y, Takada Y, Aida, K, Terahara T, Kawanishi T, Hiyama Y.	Non-destructive analysis of tulobuterol crystal reservoir-type transdermal tapes using near infrared spectroscopy and imaging,	*J Pharm Biomed Anal.*	74	14-21	2013
Endo M, Niimi S	Determination of the relative light scattering intensity of aggregates induced by stirring of humanized monoclonal antibody product using dynamic light scattering	衛研報告	130	43-45	2012
川西徹	第16改正日本薬局方製剤総則における「経口投与される製剤」および「口腔内に適用する製剤」－口腔内崩壊錠の位置づけ－	ファームテックジャパン	48	119-123	2012
川西 徹	日本薬局方の今とこれから	ファルマシア	28	20-25	2012
川西 徹	医薬品の品質を巡る話題　－化学合成医薬品に関わるレギュラトリーサイエンス－	レギュラトリーサイエンス誌	2	67-73	2012
川崎ナナ，石井明子	抗体医薬品のバイオ後続品の将来展望	臨床と微生物	39	459-465	2012
川崎ナナ，石井明子	バイオ後続品	日本病院薬剤師誌	48	1079-1086	2012

石井明子，原園景，川崎ナナ	バイオ後続品／バイオシミラーに関する国内外の規制動向と品質評価	ファームテクジャパン	**29**		2013
小椋康光	ICP-AESとICP-MSの一般試験法への新規収載	ファームテクジャパン	**28**	2791-2794	2012

International Journal of Pharmaceutics 423 (2012) 401–409

Contents lists available at SciVerse ScienceDirect

International Journal of Pharmaceutics

journal homepage: www.elsevier.com/locate/ijpharm

Pharmaceutical nanotechnology

Evaluation of intracellular trafficking and clearance from HeLa cells of doxorubicin-bound block copolymers

Kumiko Sakai-Kato[a,*], Keiko Ishikura[a], Yuki Oshima[a], Minoru Tada[b], Takuo Suzuki[b], Akiko Ishii-Watabe[b], Teruhide Yamaguchi[c], Nobuhiro Nishiyama[d], Kazunori Kataoka[d,e], Toru Kawanishi[c], Haruhiro Okuda[a]

[a] Division of Drugs, National Institute of Health Sciences, 1-18-1 Kamiyoga, Setagaya-ku, Tokyo 158-8501, Japan
[b] Division of Biological Chemistry and Biologicals, National Institute of Health Sciences, 1-18-1 Kamiyoga, Setagaya-ku, Tokyo 158-8501, Japan
[c] National Institute of Health Sciences, 1-18-1 Kamiyoga, Setagaya-ku, Tokyo 158-8501, Japan
[d] Center for Disease Biology and Integrative Medicine, Graduate School of Medicine, The University of Tokyo, 7-3-1 Hongo, Bunkyo-ku, Tokyo 113-0033, Japan
[e] Department of Materials Engineering, Graduate School of Engineering, The University of Tokyo, 7-3-1 Hongo, Bunkyo-ku, Tokyo 113-8656, Japan

ARTICLE INFO

Article history:
Received 1 July 2011
Received in revised form
16 November 2011
Accepted 15 December 2011
Available online 23 December 2011

Keywords:
Doxorubicin-bound block copolymers
Intracellular trafficking
Confocal microscopy
Transporter
Endocytosis

ABSTRACT

New technologies are needed to deliver medicines safely and effectively. Polymeric nanoparticulate carriers are one such technology under investigation. We examined the intracellular trafficking of doxorubicin-bound block copolymers quantitatively and by imaging doxorubicin-derived fluorescence using confocal microscopy. The polymers were internalized by endocytosis and distributed in endosomal/lysosomal compartments and the endoplasmic reticulum; unlike free doxorubicin, the polymers were not found in the nucleus. Moreover, the ATP-binding cassette protein B1 (ABCB1) transporter may be involved in the efflux of the polymer from cells. This drug delivery system is attractive because the endogenous transport system is used for the uptake and delivery of the artificial drug carrier to the target as well as for its efflux from cells to medium. Our results show that a drug delivery system strategy targeting this endogenous transport pathway may be useful for affecting specific molecular targets.

1. Introduction

Recently, genomic drug discovery techniques, organic synthesis, and screening technologies have been used to develop molecularly targeted medicines, some of which are already being used clinically (Hopkins and Groom, 2002; Hughes, 2009). However, these new technologies do not necessarily lead to the introduction of new treatments because even when promising compounds are discovered by genomic drug discovery techniques, they often have harmful properties or are difficult to deliver to the target because they are relatively insoluble (Hopkins and Groom, 2002; Lipinski et al., 2001). New formulation technologies are being developed to enhance the effectiveness and safety of pharmaceutical products by focusing on improving the release, targeting, and stability of drugs within the body, so that the location and timing of their action in the living body can be controlled.

Nanotechnological advances have contributed to the development of new drug delivery system (DDS) products such as polymeric micelles and liposomes that range in size from several tens of nanometers to 100 nm (Ferrari, 2005). Some of these DDS products are already being marketed as innovative medical treatments (O'Brien et al., 2004), and the number being used in clinical trials has risen impressively in recent years (Hamaguchi et al., 2007; Kuroda et al., 2009; Matsumura et al., 2004). These nanoparticulates possess several unique advantages for drug delivery, including high drug-loading capacity, controlled drug release, and small size, which allows the drug to accumulate in pathological tissues such as tumors, which have increased vascular permeability (Nishiyama and Kataoka, 2006).

Polymeric micelles have received considerable attention recently as promising macromolecular carrier systems (Allen et al., 1999; Kataoka et al., 1993, 2001; Lavasanifar et al., 2002; Torchilin, 2002; Torchilin et al., 2003). Polymeric micelles are amphipathic systems in which a hydrophobic core is covered with an outer

Abbreviations: DDS, drug delivery system; PEG, polyethyleneglycol; RES, reticuloenodothelial system; EPR, enhanced permeability and retention; Dox, doxorubicin; DMEM, Dulbecco's modified Eagle's medium; FBS, fetal bovine serum; DLS, dynamic light scattering; AFM, atomic force microscopy; HBSS, Hank's balanced salt solution; ER, endoplasmic reticulum; ECFP, enhanced cyan fluorescent protein; Alexa-transferrin, Alexa Fluor 488 conjugate of transferrin; MTOC, microtubule-organizing center; ABCB1, ATP-binding cassette protein B1; MDR1, multidrug resistance 1; (PBS), phosphate-buffered saline; EDTA, ethylenediamine tetraacetic acid; SDS, sodium dodecyl sulfate; PVDF, polyvinylidene fluoride.

* Corresponding author. Tel.: +81 3 3700 9662; fax: +81 3 3700 9662.
E-mail address: kumikato@nihs.go.jp (K. Sakai-Kato).

0378-5173/$ – see front matter © 2011 Elsevier B.V. All rights reserved.
doi:10.1016/j.ijpharm.2011.12.022

shell consisting of hydrophilic macromolecules such as polyethylene glycol (PEG) chains. Polymeric micelles can both encapsulate medicine of high density and evade the foreign body recognition mechanism within the reticuloendothelial system (RES), and they show excellent retention in the blood (Illum et al., 1987). In addition, accurate size control of the nanoparticulates enables them to accumulate in cancerous tissue, owing to the increased permeability of tumor vessels due to the enhanced permeability and retention (EPR) effect (Matsumura and Maeda, 1986).

To maximize the efficacy and safety of DDS products, it is important to deliver these products to specific target cells and subcellular compartments. In the experiments reported here, we used confocal microscopy to study the intracellular trafficking of polymeric nanoparticulate carriers. The use of covalently bound fluorescent reagents as probes is gradually clarifying the internalization pathways and intracellular localizations of polymeric nanoparticulate carriers (Lee and Kim, 2005; Manunta et al., 2007; Murakami et al., 2011; Rejman et al., 2005; Richardson et al., 2008; Sahay et al., 2008; Savić et al., 2003). However, the excretion of the polymers from target cells after they have released the incorporated drugs has not yet been clarified in detail, although information about the clearance of carriers from cells is important from the perspective of safety. In this study, we examined the trafficking of a polymeric nanoparticulate carrier in detail, including the efflux of the polymers from cells to medium, by direct measurement of doxorubicin (Dox) covalently bound to the block copolymer. This technique avoids the necessity of considering the effects of exogenously tagged fluorescent probes on the intracellular trafficking.

Dox is one of the most effective available anticancer drugs in spite of its severe toxic effects, especially cardiotoxicity (Olson et al., 1988). As the carrier we used a PEG-poly(aspartic acid) block copolymer with covalently bound Dox (Fig. 1) (Yokoyama et al., 1999), because Dox has relevant hydrophobicity to form globular micelles by means of the hydrophobic interactions, and inherent fluorescence to investigate the intracellular trafficking of the carrier itself. Dox is partially covalently bound to the side chain of the aspartic acid (about 45% of aspartic acids), so that prepared Dox-conjugated block copolymers show good Dox entrapment efficiency possibly due to the π–π interaction between conjugated and incorporated Dox molecules (Bae and Kataoka, 2009; Nakanishi et al., 2001). Therefore, in this carrier system, there are two kinds of Dox; one is Dox covalently bound to block copolymers, and the other is free Dox which is incorporated in the inner core and has a pharmacological activity by its release from the inner core. The inner core of the micelles is greatly hydrophobic owing to the conjugated Dox, while the PEG of the outer layer prevents uptake by the RES. The resulting micelle effectively accumulates in tumor tissue by the EPR effect and shows much stronger activity than free Dox (Nakanishi et al., 2001). Because the block copolymer can form globular micelles by means of hydrophobic interactions with the conjugated Dox, as shown in Section 3.1, we used a carrier without incorporated free Dox to investigate the intracellular trafficking of the carrier itself. Furthermore, by quantifying directly the amount of Dox covalently bound to the polymers, we could measure the intracellular amount of the polymers.

2. Materials and methods

2.1. Cells and micelles

HeLa cells (Health Science Research Resources Bank, Osaka, Japan) were kept in Dulbecco's modified Eagle's medium (DMEM; Invitrogen Corp., Carlsbad, CA, USA) supplemented with 10% fetal bovine serum (FBS; Nichirei Biosciences Inc., Tokyo, Japan) and 100 U/mL penicillin/streptomycin (Invitrogen). Cells were grown in a humidified incubator at 37 °C under 5% CO_2. Dox-bound polymeric micelles and fluorescent dye (DBD)-labeled PEG-polyaspartate block copolymers partially modified with 4-phenyl-1-butanol were synthesized by Nippon Kayaku Co. Ltd. (Tokyo, Japan) (Nakanishi et al., 2001).

2.2. Physicochemical data of Dox-bound micelles

The diameters and distribution of micelles were determined by using dynamic light scattering (DLS; Zetasizer Nano ZS, Malvern, UK) at 25 °C. The micelles were dissolved in water and filtered through a 0.2-μm filter before measurement. Atomic force microscopy (AFM) measurements were conducted with a NanoWizard II (JPK Instruments, Berlin, Germany) at room temperature. Images were obtained in tapping mode using a commercial microcantilever with a spring constant of 150 N/m (Olympus Corporation, Tokyo, Japan). AFM images were processed with SPM image processing v. 3 software from JPK Instruments.

2.3. Quantitation of Dox-bound polymers in HeLa cells

The amounts of Dox-bound polymers in HeLa cells were determined by measuring the amount of doxorubicinone, which is released by acid hydrolysis of Dox-bound polymers (Fig. 1b). HeLa cells (1.5×10^5) were plated in 35-mm glass-bottom dishes coated with poly-L-lysine (Matsunami, Osaka, Japan) in DMEM containing 10% FBS and 100 U/mL penicillin/streptomycin. After incubation for two days (37 °C, 5% CO_2), the cells were exposed to 50 μg/mL Dox-bound polymers in culture medium. After the indicated durations, the cells were washed and kept in phosphate-buffered saline (PBS) or Hank's balanced salt solution (HBSS; Invitrogen). The cells were trypsinized with 0.25% trypsin-ethylenediamine tetraacetic acid (EDTA) (Invitrogen) and collected. Cells were then washed with PBS three times, and a small part of the cell suspension was used for cell counting. After centrifugation at 1000 rpm for 5 min, cell pellets were resuspended in 100 μL PBS, and the suspension was divided into two parts (50 μL was used with acid hydrolysis and 50 μL without) and stored at −80 °C until analysis. After thawing, the cell suspensions were disrupted by ultrasonic liquid processor (ASTRASON 3000, Misonix, NY, USA) for 1 min. Then, 50 μL of suspension was hydrolyzed by 0.5 N HCl at 50 °C for 15 h. After hydrolysis, samples were deproteinized with methanol, followed by centrifugation at 15,000 × *g* for 5 min at 4 °C. The supernatant was then neutralized with ammonium buffer, and evaporated to dryness under reduced pressure (Savant SpeedVac concentrator, Thermo Fisher Scientific, MA, USA). The residues were resuspended in 60% methanol, and the doxorubicinone released from the polymers by acid hydrolysis was quantified by ultra-high-performance liquid chromatography by using our previously reported method (Sakai-Kato et al., 2010) to determine the amount of intracellular Dox-bound polymers (Fig. 1b). The other 50 μL of cell suspension was treated in the same way but without the hydrolysis step to evaluate the amount of free doxorubicinone, that is, doxorubicinone not derived from Dox-bound polymers. The results of three independent experiments were averaged and analyzed statistically by *t*-test.

2.4. In vitro cytotoxicity

HeLa cell lines were evaluated in the present study. The HeLa cells were maintained in monolayer cultures in DMEM containing 10% FBS and 100 U/mL penicillin/streptomycin. WST-8 Cell Counting kit-8 (Dojindo, Kumamoto, Japan) was used for cell proliferation assay. 3000 cells of HeLa cell line in 100 μL of culture medium were plated in 96 well plates and were then incubated for 24 h at 37 °C. Serial dilutions of Dox-bound polymers, micelles incorporating free Dox or just free Dox were added, and the cells were incubated for 24

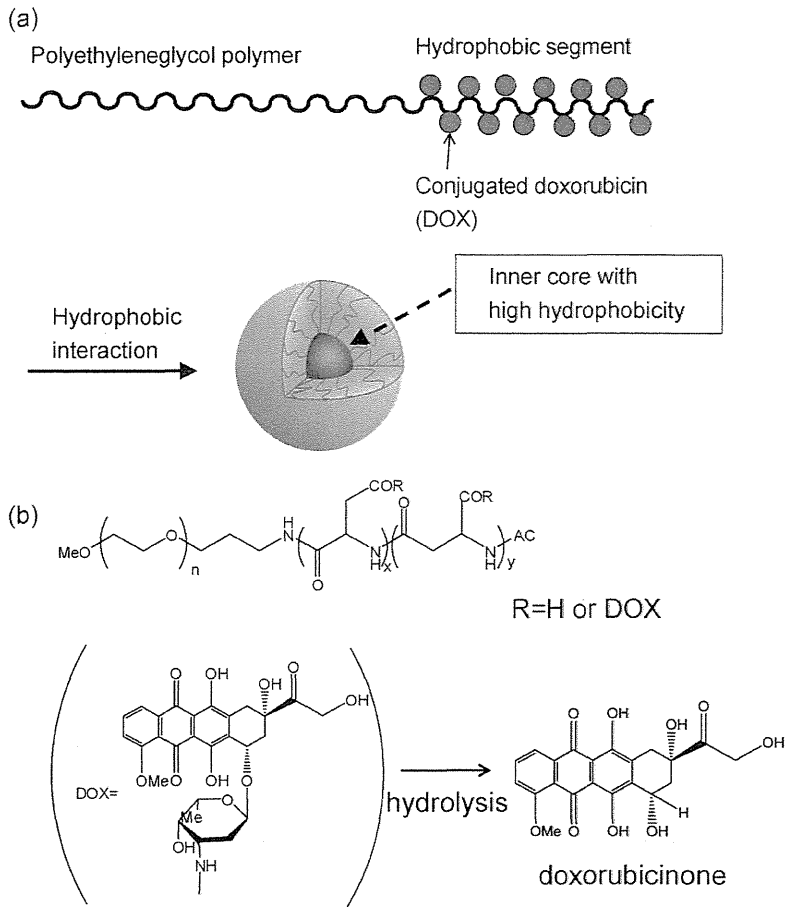

Fig. 1. Schematic of the structure of a Dox-bound polymeric micelle (a) and the chemical structure of the block copolymer (b). Polymer-bound Dox can be released as doxorubicinone by acid hydrolysis. The quantity of released doxorubicinone was used as a measure of the amount of intracellular polymers.

or 48 h. All data were expressed as mean ± SD of triplicate data. The data were then plotted as a percentage of the data from the control cultures, which were treated identically to the experimental cultures, except that no drug was added.

2.5. Confocal analysis of live cells

The intracellular trafficking of the Dox-bound micelles in live cells was examined by confocal microscopy (Carl Zeiss LSM 510, Oberkochen, Germany, or Nikon A1, Tokyo, Japan). Data were collected using dedicated software supplied by the manufacturers and exported as tagged image files (TIFs). HeLa cells (1.5×10^5) were plated in 35-mm glass-bottom dishes coated with poly-L-lysine (Matsunami) in DMEM containing 10% FBS and 100 U/mL penicillin/streptomycin. After incubation for two days (37 °C, 5% CO_2), the cells were exposed to 50 μg/mL Dox-bound polymers in culture medium. After the indicated durations, the cells were washed and kept in PBS or HBSS (Invitrogen) for imaging with the confocal microscope.

2.6. Labeling specific organelles in live cells

After incubation with Dox-bound polymers for 24 h, HeLa cells were washed with HBSS and labeled with organelle-specific fluorescent probes in accordance with the manufacturer's instructions. LysoTracker probe (Invitrogen) was used for labeling lysosomes, and ER-Tracker (Invitrogen) was used for labeling the endoplasmic reticulum (ER). A fluorescent Alexa Fluor 488 conjugate of transferrin (Alexa-transferrin; Invitrogen) was used as an exogenously added endocytic marker to delineate the endocytic recycling pathway for live cell imaging.

We also used an expression construct containing enhanced cyan fluorescent protein (ECFP) fused to an Golgi-targeting sequence derived from human β-1,4-galactosyltransferase as an Golgi localization marker (ECFP-Golgi). The construct was purchased from Clontech (Takara Bio Inc., Shiga, Japan). Cells were grown in 35-mm glass-bottom dishes coated with poly-L-lysine and transfected with Lipofectamine 2000 (Invitrogen). After overnight incubation, the cells were exposed to and allowed to internalize Dox-bound micelles for 24 h and then examined with confocal microscopy.

2.7. Efflux study of DOX-bound polymers or DBD-labeled polymers using the ABCB1 inhibitor verapamil

HeLa cells (1.5×10^5) were plated in 35-mm glass-bottom dishes coated with poly-L-lysine in DMEM containing 10% FBS and 100 U/mL penicillin/streptomycin. After incubation for two days (37 °C, 5% CO_2), the cells were exposed to 50 μg/mL Dox-bound polymers in culture medium for 3 h. Cells were washed with 50 μg/mL verapamil (Wako Pure Chemical Industries, Ltd., Osaka, Japan) (Davis et al., 2004; Kolwankar et al., 2005) or 0.1% dimethyl sulfoxide as a control. After washes, the cells were incubated for another 2 h in HBSS containing the same concentration of reagent. The cells were collected and processed for measurement of intracellular concentrations of Dox-bound polymers as described in Section 2.3. The efflux of DBD-labeled polymers was evaluated by

measurement of the fluorescent intensity inside cells using confocal microscopy. The intensity of the intracellular fluorescence was evaluated by image processing software (MetaMorph, Molecular Devices, CA, USA). The intensity of a single cell was mathematically determined by dividing the total intensity by the number of cells. Three independent experiments were averaged and analyzed statistically with the *t*-test.

2.8. Knockdown of ABCB1 by siRNA

Stealth RNAi oligonucleotides (Invitrogen) were used for siRNA experiments. Human ABCB1-siRNA sense, 5′-UCCCGUAGAAACCUUACAUUUAUGG-3′, and antisense, 5′-CCAUAAAUGUAAGGUUUCUACGGGA-3′, sequences were used. For a negative control, the Stealth RNAi Low GC Negative Control Duplex (Invitrogen) was used. The Stealth RNAi oligonucleotides were transfected into HeLa cells by using Lipofectamine RNAi MAX according to the manufacturer's protocols. After two days, the cells were exposed to 50 μg/mL Dox-bound polymers in culture medium for 3 h. After incubation, cells were washed with HBSS, and then incubated for another 2 h in HBSS without polymers. Cells were collected, and the intracellular polymers were quantified as described in Section 2.3.

2.9. Western blotting

Cells were washed with PBS and lysed in lysis buffer (20 mM Tris-HCl, pH 7.5; 1 mM EDTA; 10% glycerol; and 1% Triton X-100) containing protease inhibitors, namely, 2 mM phenylmethylsulfonyl fluoride and protease inhibitor cocktail (Sigma-Aldrich, St. Louis, MO, USA). Samples were electrophoresed on a sodium dodecyl sulfate (SDS)-polyacrylamide gel (5–20%) and transferred to a Polyvinylidene fluoride (PVDF) membrane. The blots were probed with anti-MDR (G-1) antibody (Santa Cruz Biotechnology, Inc., Santa Cruz, CA, USA) and developed with anti-mouse IgG peroxidase-linked species-specific whole antibody (from sheep) (GE Healthcare UK Limited, Little Chalfont, UK) by chemiluminescence.

3. Results and discussion

3.1. Physicochemical properties of Dox-bound micelles

The micelle carrier (Fig. 1) consisted of a block copolymer of PEG (molecular weight about 5000) and poly(aspartic acid) (polymerization degree, 30). To increase the hydrophobicity of the inner core, Dox was partially conjugated (about 45%) to the side chain of the aspartic acid. Because particle size affects the intracellular uptake of nanoparticulate formulations, we first examined the particle size of the micelles without free Dox. The Dox-bound micelles had a hydrodynamic diameter of about 42 nm at the dosed concentration of 50 μg/mL (Fig. 2a). AFM measurement of the micelles also confirmed that they were spherical with a particle size of around 40 nm (Fig. 2b). This size of micelle without free Dox is very similar to that of the micelles containing free Dox in the inner core that interacts with the conjugated Dox (Nakanishi et al., 2001), indicating that the presence of incorporated free Dox does not change the average diameter much.

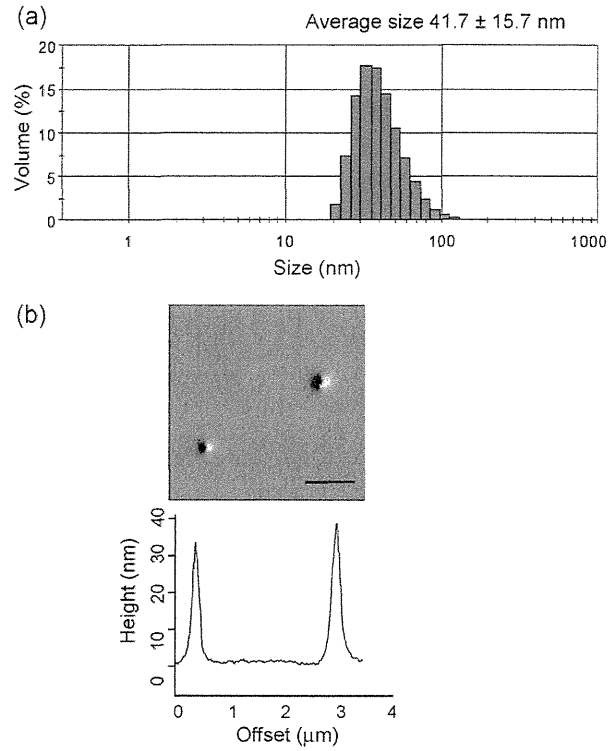

Fig. 2. Physicochemical properties of Dox-bound polymeric micelles. (a) Average size distribution of Dox-bound polymeric micelles by DLS. (b) The upper image shows an AFM image of Dox-bound polymeric micelles (bar: 1 μm) and the lower shows the cross-sectional topological profile of the image drawn in the upper panel.

3.2. In vitro cytotoxicity

We examined the *in vitro* cytotoxicity of the Dox-bound copolymers and the micelles incorporating free doxorubicin. As shown in Table 1, the cytotoxicity of doxorubicin-bound copolymers was negligible. This fact has been also reported in the previously published paper (Nakanishi et al., 2001). On the other hand, micelles incorporating free doxorubicin showed equivalent *in vitro* cytotoxic activity to free doxorubicin which is not incorporated into micelle. Therefore, in this system, the doxorubicin was conjugated to the block copolymer to increase the hydrophobicity of the inner core of the micelle so that efficient amount of free doxorubicin can be incorporated into the inner core of the micelles, and its cytotoxicity was negligible.

3.3. Intracellular uptake of Dox-bound polymers

To evaluate the intracellular uptake of Dox-bound polymers, we measured their intracellular amount by quantitating the doxorubicinone released from the intracellular polymers by acid hydrolysis treatment (Fig. 1b). Although the Dox-bound polymers contained 0.02% (w/w) free doxorubicinone as an impurity, no inherent free doxorubicinone was detected in the cells in any of the experiments in which we measured the intracellular concentration of doxorubicinone without acid hydrolysis. This result also indicates that

Table 1
IC50 values (μg/mL).

24 h			48 h		
Dox-bound polymer	Micelle incorporating free Dox	Free Dox	Dox-bound polymer	Micelle incorporating free Dox	Free Dox
>10	0.37	0.27	>10	0.045	0.024

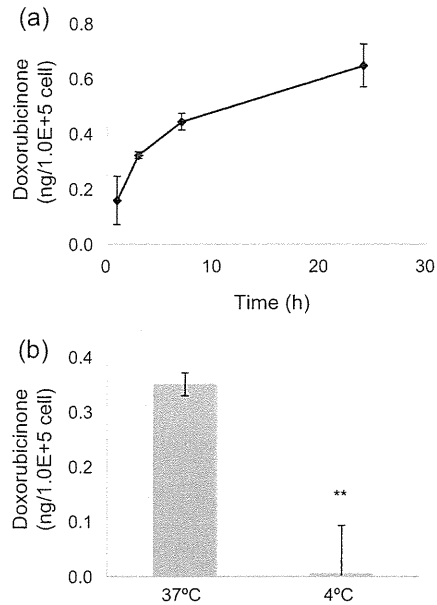

Fig. 3. Internalization of Dox-bound polymers. (a) Change in the internalized amount of Dox-bound polymers in cells as indicated by released doxorubicinone over time. HeLa cells were incubated in medium containing Dox-bound polymers for the indicated durations, followed by washes with PBS. The doxorubicinone released by acid hydrolysis was quantitated as a measure of the amount of intracellular polymers, as described in Section 2. (b) Effect of temperature on the internalization of Dox-bound polymers. HeLa cells were incubated in medium containing Dox-bound polymers at 37 °C or 4 °C for 3 h, followed by washes with PBS. The amount of intracellular polymers was quantitated by measuring the doxorubicinone released by acid hydrolysis, as described in Section 2. $^{**}P < 0.01$.

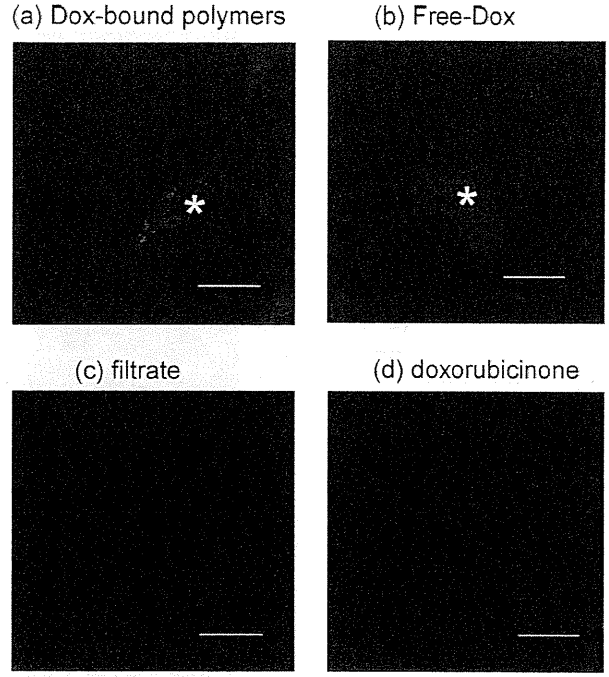

Fig. 4. Intracellular distribution of (a) DOX-bound polymers in HeLa cells exposed to 50 μg/mL Dox-bound polymers and (b) free DOX in cells exposed to 5 μg/mL free Dox for 1 h. Intracellular distribution of DOX-bound polymers in HeLa cells (c) cultured for 24 h in medium containing the filtrate of medium that was preincubated with Dox-bound polymers, and (d) cultured with 20 ng/mL free doxorubicinone for 24 h. Bars: 10 μm. Asterisk indicates the nucleus.

degradation of Dox-bound polymers that releases doxorubicinone during the experiments was negligible.

We then incubated HeLa cells in medium containing Dox-bound polymers for 1–24 h. After the incubation, the cells were washed. By determining the amounts of doxorubicinone released from Dox-bound polymers by acid hydrolysis of the cells, we were able to observe a time-dependent increase in the intracellular amount of Dox-bound polymers (Fig. 3a). Moreover, the amount of polymers in cells was significantly lower in cells incubated with the polymers at 4 °C than at 37 °C (Fig. 3b), indicating that the cells took up the polymers by endocytosis.

3.4. Intracellular distribution of Dox-bound polymers

The intracellular distribution of Dox-bound polymers was studied by confocal microscopy using the inherent fluorescence of the Dox covalently bound to the block copolymers. The Dox-bound polymers were localized in the perinuclear regions but not in the nucleus (Fig. 4a). This was different from the localization of free Dox which was distributed in the nucleus after 1 h (Fig. 4b), as reported previously (Beyer et al., 2001). This distribution will explain the fact that *in vitro* cytotoxicity of Dox-bound polymers was negligible (Table 1). To confirm that the Dox was not released from block copolymers as doxorubicinone (Fig. 1b) during the incubation time of the experiment, Dox-bound polymers were incubated in cell culture medium for 1 h at 37 °C, and then removed by centrifugal filtration using a Microcon YM-3 tube (Millipore, MA, USA). The resultant filtrate was added to the cell culture medium. Confocal microscopy showed no fluorescence within the cells (Fig. 4c). Furthermore, when HeLa cells were cultured in cell culture medium containing 20 ng/mL free doxorubicinone, which corresponds to 0.02% (w/w) of Dox-bound polymers, for 24 h, fluorescence was negligible within the cells (Fig. 4d). These results show that the fluorescence seen within the cells after Dox-bound polymer incubation is caused by the uptake of polymers and not by free doxorubicinone or Dox.

We next examined the intracellular localization of Dox-bound polymers by colocalization studies using fluorescent organelle markers. The fluorescence derived from Dox-bound polymers coincided well with the specific staining of the ER by ER-Tracker in double-labeling experiments (Fig. 5a). High-resolution images showed that both staining procedures clearly stained membranal structures (Fig. 5b).

Because the Golgi apparatus is also located in the perinuclear area and is involved in the intracellular transport of various molecules, we investigated the localization of the polymers by transfecting cells with an expression construct containing ECFP fused to a Golgi-specific protein. As shown in Fig. 5c, the distribution of polymers in the Golgi was negligible. We also confirmed that treatment of cells with Lipofectamine treatment did not affect the distribution of polymers (data not shown).

To what, then, can this particularly strong staining of the perinuclear areas be attributed? The perinuclear area is known to be the microtubule-organizing center (MTOC), an area in eukaryotic cells from which microtubules emerge and where endosomes and other endocytotic vesicles cluster (Matteoni and Kreis, 1987). In fact, a fluorescent staining image showed that the vesicles containing Dox-bound polymers in the perinuclear area (Fig. 6a, yellow arrows) coincided with the MTOC, as marked by Alexa-transferrin, an endocytic marker (Fig. 6a, white arrows). Some of the vesicles containing polymers were also stained by LysoTracker, a dye that specifically stains lysosomes (Fig. 6b). These results show that the polymers are internalized by endocytosis and transported to endosomal/lysosomal compartments. Duncan and colleagues, examined the localization of polymers by using Oregon Green as a fluorescent tag and found that three water-soluble polymeric carriers, *N*-(2-hydroxypropyl)methacrylamide, Dextran, and PEG, localized to late